Passive Scalar Mixing Downstream of a Synthetic Jet in Crossflow

Glen Mitchell[1], Emmanuel Benard[1], Vaclav Uruba[2], and Richard .K. Cooper[1]

[1] School of Mechanical and Aerospace Engineering, Queen's University Belfast, Belfast, UK
[2] Institute of Thermomechanics, The Academy of Sciences of the Czech Republic, Prague, Czech Republic

1 Introduction

Surface heat transfer is important in many engineering applications, e.g. energy, aerospace and automotive. For a crossflow, it is possible to increase surface heat transfer through the use of vortex generators upstream of the heat transfer surface [1, 2] and by injecting continuous jets into the flow [3]. In both cases, heat transfer enhancement is obtained by altering the thermal mixing near the surface. It is possible that a synthetic jet could also be used to improve crossflow surface heat transfer.

The synthetic jet actuator consists of a cavity with an oscillating surface acting as one wall and an orifice in another wall. During the forced oscillation of the surface, fluid is alternately entrained into and expelled from the cavity creating a series of vortex pairs that coalesce to form a jet. In a cross-flow, the vortex generated travels downstream of the orifice and at low ratios of jet to crossflow velocity, the vortex remains close to the wall. This vortex influences the transport of fluid within the boundary layer and, when the wall is heated, the thermal mixing.

The current study aims at investigating the influence of a 2D synthetic jet on passive scalar mixing in a turbulent boundary layer, with temperature acting as the passive scalar. An initial particle image velocimetry (PIV) study is used to study the hydrodynamics of the jet/crossflow interaction and proper orthogonal decomposition (POD) of the flow field is used to identify the conditions for near wall mixing. A laser induced fluorescence (LIF) study is then conducted in order to examine the thermal mixing due to the jet/crossflow interaction.

2 Water channel and synthetic jet actuator

The experiments were conducted in a closed circuit horizontal water channel with a test section of length 1000mm and cross-section 60mm wide by 360mm high.

The channel has a maximum test section velocity of 40cm/s with a freestream turbulence intensity of less than 1.5%. The flow along the sidewall of the channel was tripped just after the contraction using cylindrical roughness elements to generate a turbulent boundary layer. The boundary layer can be heated by a 400mm long copper plate. The plate is located 600mm downstream from the start of the test section and has two uniform heat flux electrical heaters at the rear. A radiator in the settling chamber of the channel ensures the water temperature fluctuates by less than 0.1°C.

The synthetic jet was generated by a mechanical piston/cylinder arrangement connected to a cavity with a slot type orifice of width 0.75mm and length 105mm. The jet orifice is located in the heated copper plate, 130 slot widths downstream from the start of the thermal boundary layer and is orientated so the long axis of the orifice is perpendicular to the flow. An electromagnetic shaker is used to excite the piston with a sinusoidal oscillation. The cylinder is connected to the cavity by a flexible hose to isolate the vibration of the shaker from the channel. Using this arrangement, jets can be generated with Reynolds number ranging from 20 to 1000 and Strouhal numbers in the range 0.001 to 0.2.

3 PIV/LIF technique

The PIV/LIF system consists of a 15Hz double pulsed Nd:YAG (532nm wavelength) laser and a CCD camera with a resolution of $2048 \times 2048 \text{pixels}^2$ and a maximum frame rate of 15 frames per second. The laser light sheet was adjusted so it was located along the orifice centreline parallel to the flow and the flow was seeded with hollow glass spheres for PIV and Rhodamine B fluorescent dye for the LIF temperature measurements.

For both the PIV and LIF experiments phase and ensemble averaged results were obtained. The image acquisition was phase-locked to the actuator motion with images acquired at 24 equally spaced intervals during the actuator cycle. For PIV, 150 double framed images were acquired for each phase of the cycle. These images were analysed using a multi-pass cross-correlation technique producing vector fields with a resolution of $0.22 \times 0.22\text{mm}^2$. For LIF, 40 single frame images were taken at each phase. For each image, the florescence intensity was averaged over cells of $10 \times 10\text{pixels}^2$ to maximise the signal to noise ratio resulting in a spatial resolution of 0.16×0.16mm. The intensity distribution across the light sheet varies for each laser shot. This intensity variation was corrected by a procedure similar to the correction method of Seutiëns et al [4]. The final temperature field was calculated from the florescence intensity using a pre-determined calibration relationship.

4 Proper orthogonal decomposition

The POD provides an energy efficient decomposition of the fluctuating part of the velocity field. The instantaneous velocity field is decomposed into a time

averaged component and a fluctuating component:

$$\overrightarrow{u}(\overrightarrow{x},t) = \overrightarrow{U}(\overrightarrow{x}) + \sum_{n=1}^{N} a_n(t)\phi_n(\overrightarrow{x}) \tag{1}$$

where the fluctuating component is described by a linear combination of modes, ϕ. The modes are organised so the first mode contain the most energy and the last mode the least energy. This makes POD a useful tool for identifying dominant coherent flow patterns. In this paper, the POD has been performed by the method of snaphots [5].

5 Hydrodynamic effects

To investigate the hydrodynamic effects of the interaction of the synthetic jet with a crossflow, eight different cases were studied. Only two representative cases are presented here. Case 1 has a low jet to crossflow velocity ratio and case 2 has a high velocity ratio. The parameters for both jets are given in Table 1. For both cases, the boundary layer had the following parameters at the jet orifice; $\mathrm{Re}_\theta = 760$, $\delta = 21$mm and $\mathrm{H} = 1.3$. To confirm that the boundary layer was turbulent, the velocity profile was compared to the logarithmic law of the wall and the turbulence intensity profile was examined.

The first three POD modes for each case are shown in Figure 1. It can be seen that modes 1 and 2 are similar for each case. The first mode has as structure similar to the ejection portion of the jet cycle, with a large velocity magnitude at the orifice exit and a vortex immediately downstream. The structure of the second mode resembles the suction portion of the cycle, with a smaller velocity around the orifice and the vortex further downstream. A closer look at the relationship between these two modes shows a 90° phase difference between them. Reconstructions of the flow field using these two modes are similar to the phase averaged flow, as demonstrated in Figure 2 for case 2. It should be noted that this is not valid for the start of the expulsion cycle. At this point, the two mode reconstruction differs significantly from the phase averaged flow field in the region of the orifice as modes 1 and 2 do not contain enough detail to reconstruct the complex flowfield in this area. The first two modes combined contain over 30% of the energy with subsequent modes having less than 5% each.

After the first two modes, the modes for the two jet cases start to deviate as shown in Figure 1(c). For case 1, the third mode consists of a series of vortical

Table 1. Parameters for the three jet cases considered.

Case	Re_{U0}	St_{U0}	U_∞ [cm/s]	U_0/U_∞
1	278	0.0277	40.0	0.83
2	556	0.0089	40.0	2.22
3	278	0.0089	40.0	1.11

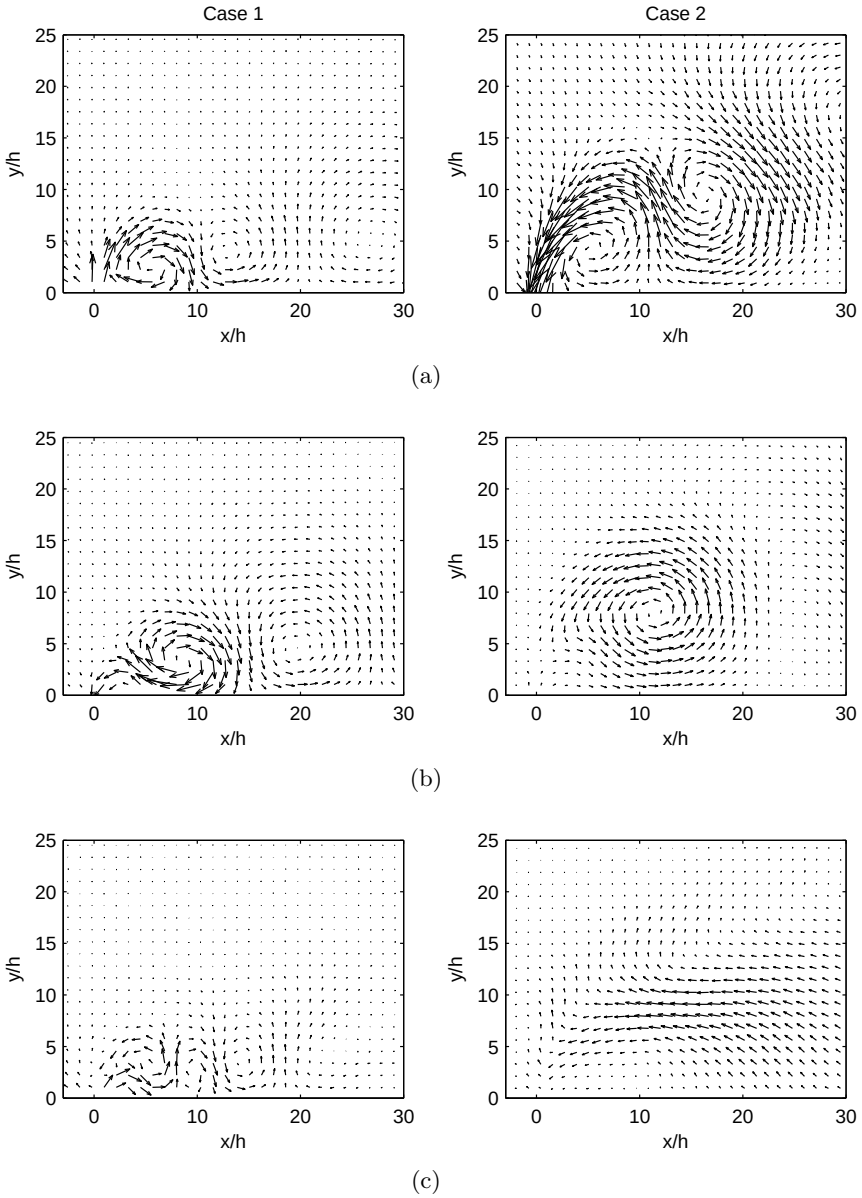

Fig. 1. Visualisation of the first three POD modes for cases 1 and 2: (a) mode 1, (b) mode 2, (c) mode 3.

structures, located close to the wall whereas case 2 has a horizontal fluctuation located away from the wall. Although not presented here, subsequent modes for case 2 tend to consist of a series of vortical motions moving away from the wall whilst, for case 1, the fluctuations in higher modes remain close to the wall.

For all eight of the jet cases studied, the POD modes followed the same pattern as cases 1 and 2. The first two modes were similar for all cases. For mode 3 and higher, the two different behaviours described above were observed. The type of behaviour the jet displays was found to be dependant on the jet to cross-flow velocity ratio. For $U_0/U_\infty < 1.2$ the fluctuations remain close to the wall whilst they move away from the wall for $U_0/U_\infty > 1.6$.

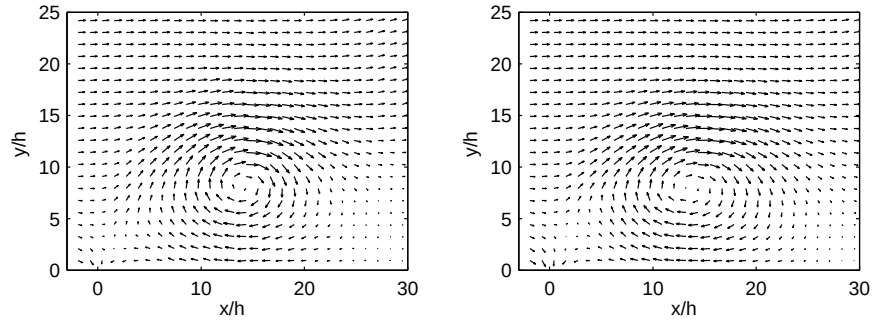

Fig. 2. The synthetic jet flowfield during the suction cycle for case 1: (a) phase-averaged, (b) 2 mode reconstruction.

6 Passive Scalar Effects

To investigate the scalar effects, a jet similar to case 1 is considered, i.e. the fluctuations in the higher modes of the POD remain close to the wall. The parameters for this jet are once again given in Table 1 (case 3). The results of the LIF study are shown in Figure 3 for two different phases of the jet cycle; half way through the ejection cycle and the midpoint of the suction cycle.

During the expulsion cycle, the jet pushes warm fluid away from the wall increasing the thickness of the thermal boundary layer downstream of the jet. Upstream of the orifice, the thermal boundary layer is unchanged from the no jet condition. During the suction cycle, the thermal boundary layer downstream of the orifice is annihilated as the jet sucks in the warm fluid close to the wall upstream of the orifice as observed in Figure 3(b). Comparing the upstream thermal boundary layers in Figures 3(a) and 3(b), it can be seen that the en-

trainment of the near wall fluid into the cavity also causes the upstream thermal boundary layer to become thinner.

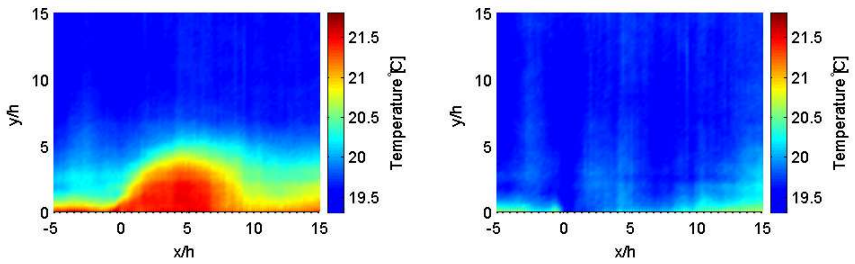

Fig. 3. Thermal mixing between the synthetic jet and a heated crossflow: (a) $t/T = 1/4$, (a) $t/T = 3/4$.

7 Conclusions

References

1. Tiggelbeck, S., Mitra, N., Fiebig, M.: Experimental investigations of heat transfer enhancement and flow losses in a channel with double rows of longitudinal vortex generators. International Journal of Heat and Mass Transfer **36** (1993) 2327–2337
2. Jacobi, A., Shah, R.: Heat transfer surface enhancement through the use of longitudinal vortices: A review of recent progress. Experimental Thermal and Fluid Science **11** (1995) 295–309
3. Zhang, X., Collins, M.: Flow and heat transfer in a turbulent boundary layer through skewed and pitched jets. AIAA Journal **31** (1993) 1590–1599
4. Seutiëns, H., Kieft, R., Rindt, C., van Steenhoven, A.: 2D Temperature Measurements in the Wake of a Heated Cylinder using LIF. Experiments in Fluids **31** (2001) 588–595
5. Sirovich, L.: Turbulence and the dynamics of coherent structures. Part I: Coherent structures. Quarterly of Applied Mathematics **45** (1987) 561–571